Journal of
Membrane Science & Technology

Caravella and Sun, J Membra Sci Technol 2016, 6:1
DOI: 10.4172/2155-9589.1000142

Research Article Open Access

Evaluation of Step Resistance in Multilayered Ceramic-Supported Pd-Based Membranes for Hydrogen Purification in the Presence of Concentration Polarisation

Caravella A[1]* and Sun Y[2]

[1]Department of Environmental and Chemical Engineering (DIATIC), University of Calabria, Via P. Bucci, Rende (CS), Italy

[2]Department of Materials Engineering, Hanyang Univeristy, Ansan, Gyeonggi-do, South Korea

Abstract

In this work, a systematic approach is used to quantify the single-step influence in composite Pd-based membranes on hydrogen permeation in the presence of concentration polarisation. To perform this study, an already developed permeation model is applied to a membrane supported on a five-layered asymmetric porous support. The results are presented in terms of both single-layer influence (calculated using an expression involving the permeation limiting fluxes) and the here introduced Support Resistance Coefficient, SRC, which is a coefficient measuring quantitatively the extent of the driving force in the entire support, analogously to what done for the definition of the Concentration Polarisation Coefficient, CPC. Analysing the membrane behaviour in different conditions of temperature, total feed pressure and Pd-layer thickness, it is eventually shows that, the presence of polarization determine a decreasing effect of the porous support in the considered configuration, i.e., with the selective layer placed on the high-pressure side and the support placed on the permeation one. This conclusion indicates that, for sufficiently thin metal layers, the hydrogen permeation is mostly influenced by concentration polarisation and, thus, the fluid dynamic conditions in the upstream side become a crucial parameter to optimise.

Keywords: Porous layers; Concentration polarisation; Palladium; Membranes; Hydrogen

Introduction

The permeation properties of composite membranes and thin films deposited on appropriate substrates and supports nowadays induce such materials to be used for a number of different industrial applications. Furthermore, multilayered structures are useful to prevent inter-diffusion between selective layers and support [1-4]. Such an interest has been boosting the development of enhanced fabrication and characterisation techniques (see, for example, refs [5-15]) adopted to optimise the membrane structure maximising the permeating flux and, dually, minimising the overall mass transfer resistance.

Zhang et al. [7] prepared a 5 micron-thick membrane with a selectivity higher than 3000, obtaining slightly lower performance than Itoh et al. [6], who deposited a thin PdAg layer of 2-4 mm with a good measured H_2/N_2 selectivity exceeding 5000, and Dittmar et al. [12], who prepared a 10-13 micron-thick membrane with variable selectivity (700-10000). Tong et al. [3] deposited a metal layer of 5 micron with virtually infinite selectivity, similarly to what done by Li et al. [5] and the research groups in SINTEF, who developed a method to sputter 2-3 mm-thick Pd-based layers on porous substrates [8,9].

Examples of ultra-thin membranes were provided by Lim et al. [10], with a 0.16 micron-thick membrane with a selectivity of around 710, and Yun et al. [11], with a membrane as thick as 1 micron within a selectivity range of 3000-9000. Furthermore, a research group of TECNALIA has recently developed a systematic methodology to prepare stable and 4-5 mm-thick selective supported Pd-based membranes [15,16]. A more exhaustive state-of-the-art on preparation and characterization of thin Pd-based membranes can be found in the recent review of Gallucci et al. [17].

Because of the high flux allowed by such thin membranes, the evaluation of the influence in the single permeation steps has been becoming progressively more important. These steps commonly include both kinetic phenomena and mass transfer, which are in general paired to each other eventually determining the overall membrane performance [18-22].

Therefore, for design purposes, a deep knowledge of the transport mechanisms involved in membranes and thin layers is required; this implying an appropriate mathematical model of the mass transfer involved in the single permeation steps.

In the particular case of hydrogen purification using membranes composed of Pd-alloy thin layers deposited on ceramic supports – which can be both symmetric and asymmetric multilayered ones – the effect of the meso-porous structure of the intermediate and top-layers can be significant, as intermediate layers and top-layer usually have a meso-structure characterised by a relatively low mean pore diameter (within [5-50] nm ca.23-29].

Furthermore, an additional permeation resistance affecting the actual membrane separation systems – and in particular the Pd-based membrane devices – is the external mass transfer resistance in the upstream mixture side, commonly named as concentration polarisation.

In the past, this phenomenon was considered not to be important

***Corresponding author:** Alessio Caravella, Department of Environmental and Chemical Engineering (DIATIC), University of Calabria, Italy; Tel: +390-984-494481; Fax: +39-0984-496655; E-mail: alessio.caravella@unical.it

Received December 21, 2015; **Accepted** January 18, 2016; **Published** January 26, 2015

Citation: Caravella A, Sun Y (2016) Evaluation of Step Resistance in Multilayered Ceramic-Supported Pd-Based Membranes for Hydrogen Purification in the Presence of Concentration Polarisation. J Membra Sci Technol 6: 142. doi:10.4172/2155-9589.1000142

in gas separation systems, as the diffusion coefficients of gases are around four orders of magnitude higher than those of liquids [30-32]. However, this hypothesis is strictly valid just for sufficiently thick selective layers providing relatively low permeating flux and, thus, with the above mentioned improvements in membrane fabrication, the state-of-the-art selective layers are sufficiently thin to provide a relatively high flux, causing the mass transport in the selective layer not to be the only permeation-determining step. Hence, a certain effect of concentration polarisation is expected in these conditions. For this reason, more complex approaches are needed to identify the permeation limiting steps, as the analysis of the support influence on permeation cannot leave aside the effect of the external mass transfer resistance, which has a direct influence on the extent of the support effect as well.

Pioneers in dividing the hydrogen permeation into several elementary steps were Ward and Dao in their modelling work [18], which involves external mass transfer, adsorption/desorption, absorption/de-absorption and internal diffusion. Later, several authors started from the Ward and Dao approach to develop more complex permeation models involving additional steps, like transport in the porous supports [20,22], concentration polarization [33-38] and external mass transfer based on a multicomponent film theory [20,21], and inhibition effects [39-42]. However, there is a lack in the existing modelling approaches to systematically relate to each other the number of mass transport phenomena playing a role in a metal membrane.

In this context, the aim of this paper is to provide a systematic way to evaluate the effect of each elementary step on permeation, showing also the mutual relationship between concentration polarisation, transport in the support and diffusion through the selective metal layer.

Description of the System

The asymmetric multilayered Pd-based membrane considered in this study (Figure 1) is similar to that considered in Caravella et al. [22]. Beside the geometrical properties of the support (Table 1), the main difference from that work is that in this paper the effect of concentration polarisation is also taken into account. For this purpose, the mixture side, which is supposed to be placed on the Pd-based layer side, is considered to be composed of four species, i.e., H_2, N_2, Ar and H_2O, whereas the pure-hydrogen side is on the support side.

With these hypotheses, the hydrogen permeation is composed of three steps: mass transport in the feed film, diffusion through the Pd-based layer and transport through the layers of the porous supports.

In the present investigation, the hydrogen content is varied independently keeping the composition ratio among the other species

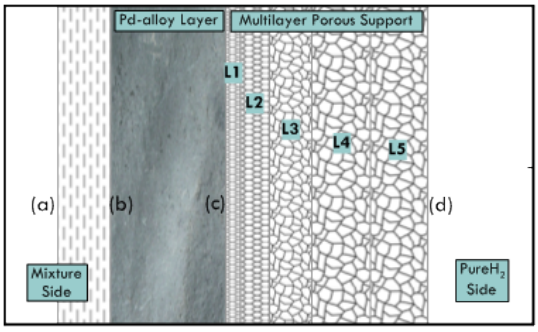

Figure 1: Sketch of the membrane considered in the present investigation.

Layer	Thickness, mm	Mean Pore Diameter, nm	Porosity, -	Tortuosity, -
1 (Top-Layer, Silica)	10	5	0.25	5
2 (g-alumina)	40	50	0.35	5
3 (a-alumina)	20	250	0.35	5
4 (a-alumina)	700	500	0.50	3
5 (a-alumina)	720	500	0.50	3

Table 1: Geometrical characteristics of the considered alumina porous support.

Side	Composition, %				Total Pressure	T_{Inlet}
	H_2	CO_2	H_2O	CO	kPa	°C
Feed	48.5	4.9	36.9	9.7	[400, 600, 800]	[300:20:400]
Sweep	100	-	-	-	[10, 20, 50]	Same as feed
ID^{Shell} = 1.2 cm, OD^{Mem} = 1 cm, d^{Shell} = 1 mm, d^{Mem} = 5 mm						

Table 2: Operating conditions considered for simulation.

constant and equal to the unity. The other operating conditions are reported in Table 2.

The multicomponent-based permeation model already introduced elsewhere is used for calculation, using the permeation properties (permeability and solubility) of a membrane characterised in a previous work accounting for the non-ideal internal hydrogen diffusion in the Pd-based layer [21,22].

Mathematical Approach

The objective of the present investigation is to provide a systematic way to evaluate the influence of the mass transfer in the porous support on the permeation process. For this purpose, two different ways of measuring the support layer effect on permeation are used.

First, the influence of the generic j^{th} permeation step (a_j) is evaluated by using the concept of limiting fluxes [22,43] (Section 4.1), reminding that the limiting flux of a particular permeation step is calculated at certain operating conditions by considering that step as the only rate determining one and all the others as they were at the equilibrium. The calculation of a_j is based on the following expression (Equation 1):

$$\alpha_j \equiv \frac{\frac{1}{J^j_{H_2,Lim}}}{\sum_{k=1}^{m}\frac{1}{J^k_{H_2,Lim}}}, \quad \sum_{j=1}^{m}\alpha_j = 1 \tag{1}$$

Where m is the number of permeation steps considered, which in this work is equal to 3 (i.e., related to external mass transfer in the feed, transport in the Pd-based layer and transport in the porous support). Equation 1 practically states that the influence of each step is given by the ratio of the limiting flux inverse of the j^{th} step divided by the sum of all the limiting flux inverses. It is remarked here that, in the particular case where all driving forces were of the same type, a_j would coincide with the more conventional resistance evaluation.

Such an approach is necessary because, in general, each permeation step is characterised by a different type of driving force (Sieverts' one, linear, quadratic and so on) and, thus, the single step resistance cannot be simply evaluated by dividing the single driving forces by flux (= inverse of permeance), as the resulting resistances would have different units and, thus, would not be comparable to each other.

In parallel to the step influence, and analogously to what done in defining an appropriate Concentration Polarisation Coefficient, CPC [35], a convenient Support Resistance Coefficient, SRC, is here

introduced to evaluate the extent of the mass transfer resistance in the support with respect to the total resistance offered by the whole supported membrane (Section 4.2). The general definition of this coefficient for each ith species is provided as follows (Equation 2):

$$SRC_i = \frac{DrivingForce_i|_{Support}}{DrivingForce_i|_{Total}} \quad (2)$$

Where the subscripts "Support" and "Total" indicate the driving force within the support and within the whole supported membrane, respectively. In the case of Pd-based membranes, only hydrogen can basically pass through and, thus, just a single SRC is needed (Equation 3):

$$SRC = \frac{DrivingForce|_{Support}}{DrivingForce|_{Total}} \quad (3)$$

The form of the characteristic driving force can be conveniently chosen based on the operating conditions, even though in most cases it is convenient to choose the Sieverts one [35], as done in the present investigation. Therefore, with reference to the notation indicated in Figure 1, Equation 3 is made explicit as reported in Equation 4:

$$SRC = \frac{\left[\sqrt{P_{H_2}^{(c)}} - \sqrt{P_{H_2}^{(d)}}\right]}{\left[\sqrt{P_{H_2}^{(a)}} - \sqrt{P_{H_2}^{(d)}}\right]} \quad (4)$$

However, as also remarked elsewhere [38], it could be convenient sometimes to choose a different driving force, such as, for example, the pressure difference or another difference of pressure functionality taking into account the non-ideality of internal diffusion in the metal lattice in terms of a pressure exponent different from 0.5 [22, 44-46].

Regarding its definition, SRC is defined in such a way that it is close to zero for negligible influence of the support, whereas it is close to the unity for support-controlled permeation. The analogy of this coefficient to CPC is clear, although there is a mathematical difference between them arising from physical reasons. In fact, in case of pure hydrogen, there is no external mass transfer resistance in the film side and, thus, there is no concentration polarisation, i.e., CPC = 0.

Differently, in the porous support there is a concentration drop owing to the effect of at least Knudsen and viscous flow, which are effective in decreasing the permeation flux even under pure hydrogen conditions. As a result, the SRC value cannot be completely zero. In this particular case, where pure hydrogen is considered in the permeation side, just Knudsen and viscous flow take place.

Before going through results and discussion of the present paper, it is useful to remark the difference between the pieces of information coming from the values of the support influence and SRC. In fact, the former provides the actual contribution of permeation steps to the overall permeation process, regardless of the particular governing driving force.

On the contrary, the latter provides the driving force loss owing to the support, which implies a choice of a characteristic driving force, as already pointed out above. In doing that, it must be considered that the farther the chosen characteristic driving force is from the actual governing one, the more sensitive SRC is to such a choice.

Results and Discussion

The subsequent sub-sections report the analysis concerning the influence of permeation steps and the support resistance coefficient under different working conditions. Although the reported quantitative results are specific for the considered conditions, the qualitative trends are general and can be studied to eventually maximise the permeating flux, which is the final objective of a membrane designer.

Permeation step influence

Figure 2 shows the calculated hydrogen profiles through membrane for different values of hydrogen mole fraction in the feed considering a total feed pressure of 1000 kPa and a temperature of 300°C. Two different cases are investigated, i.e., (a) in absence and (b) in the presence of external mass transfer resistance on the feed side (concentration polarisation).

In the former case, two permeation steps are active, i.e., Pd-alloy layer and porous support, whereas in the latter one, the external mass transfer on the feed side is additionally considered.

Considering the case without polarisation (Figure 2a), it can be observed that the majority of partial pressure drop is in the Pd-based layer, although there is a non-negligible drop in the porous support, mostly concentrated in the first two porous layers. This means that, under the considered conditions, the internal diffusion in the metal selective layer is not the only rate-determining step of the overall permeation.

Furthermore, the hydrogen profile through the metal layer is generally more than linear due to the "non-ideality" of the diffusion coefficient in the Pd-based layer, as diffusivity is an increasing function of hydrogen concentration in the conditions of interest of the present paper [44-48]. In light of such functionality, the profile non-linearity is progressively more pronounced as the hydrogen concentration increases.

This trend is shown by the dashed lines reported in Figure 2, each of which have the slope equal to that of the true profile calculated at the permeation side (low hydrogen pressure).

As for the values of the hydrogen mole fraction shown in Figure 2,

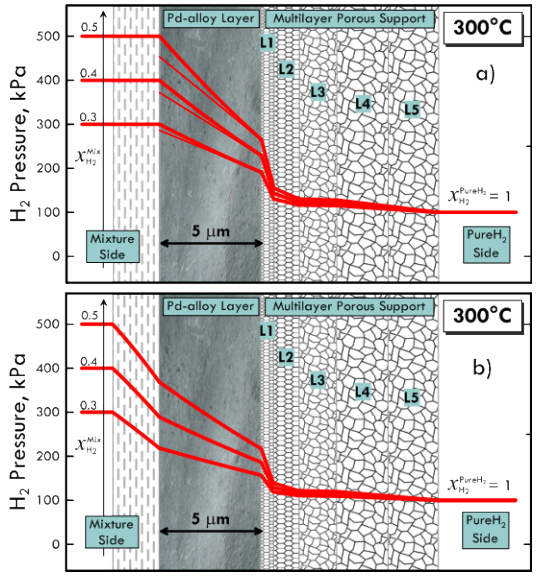

Figure 2: Hydrogen partial pressure profiles across Pd-based membranes for different values of hydrogen mole fraction in the feed a) without polarisation and b) with polarisation. Profiles in the metal layer are reported in terms of equivalent partial pressure. The dashed lines are reported to show the profile non-linearity.P^{Feed}= 1000 kPa, T = 300°C, d^{Mem}= 5 mm.

the profile non-linearity is more evident at a hydrogen mole fraction of 0.5, whilst the profiles corresponding to 0.4 and 0.3 show trends that are progressively more linear. This is due to the fact that a higher hydrogen concentration in the lattice is shown to experimentally favour the hydrogen internal diffusion, at least within a concentration range where the lattice-hydrogen interactions are dominant on the hydrogen-hydrogen ones [47].

As for the profiles in the support layer, in pure hydrogen conditions at a fixed permeate pressure, a second order functionality of the profiles with the hydrogen partial pressure is theoretically found because of the presence of both Knudsen diffusion (linear along the support) and viscous flow (quadratic trend). However, since the contribution of the viscous flow is really small in the considered conditions, the profiles in the support layers can be considered practically linear.

The situation depicted in Figure 2b is slightly different. In fact, the presence of external mass transfer resistance on the feed side causes a hydrogen partial pressure drop. As a consequence, the hydrogen concentration in the metal lattice is lower with respect to the case in absence of mass transfer resistance, this implying more linear profiles in the Pd-based selective layer. Therefore, the mass transfer resistance acts in decreasing the permeating flux in two ways: the first one, which is more direct, acts by offering an additional resistance to permeation. The second one acts to decrease the hydrogen concentration in the metal layer, causing the non-ideality effect to be weaker and, thus, a consequent lower flux.

Concerning the effect of the support, it offers a non-negligible pressure drop. However, it must be remarked that the characteristic driving forces of each permeation steps are different, i.e., approximately linear with DP_{H2} for the external mass transfer in the feed and in the support layers, and approximately linear with $\Delta P_{H_2}^{0.5}$ (Sieverts' law) in the Pd-based layer.

Therefore, the single-step influence should not be evaluated by considering the pressure drop only, as this quantity is not representative of the permeation in each step. This is the reason why the quantitative influence based on the permeating limiting flux is required [43]. To this regard, Figure 3 shows the step influence as a function of temperature at certain operating conditions, calculated in the way mentioned in the previous section.

Considering the temperature of 300°C, it is possible to notice that the influence of external mass transfer, Pd-based layer and support is around 40%, 35% and 25%, respectively. Therefore, it is not possible

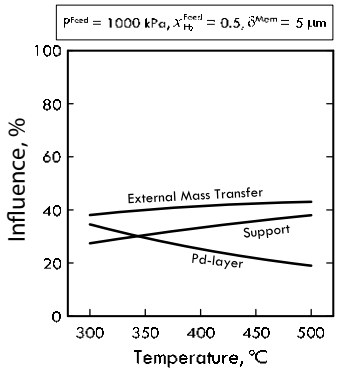

Figure 3: Step influence as a function of temperature for the three permeation steps considered in this work. P^{Feed}=1000 kPa, $x_{H_2}^{Feed}$=0.5, d^{Mem}=5 mm.

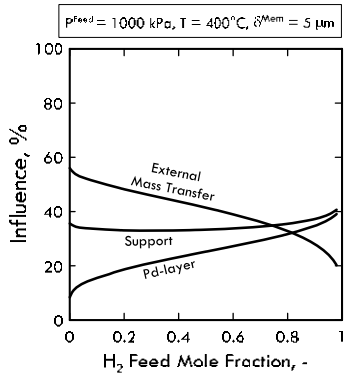

Figure 4: Step influence as a function of the hydrogen mole fraction in the feed for the three permeation steps considered in this work. P^{Feed}=1000 kPa, T=400°C, d^{Mem}=5 mm.

to recognise a single permeation-determining step. As temperature increases, the ratios of the steps rate changes, causing the relative influence to change as well.

This behaviour is related to the fact that temperature favours the activated processes, which, thus, becomes progressively faster with increasing temperature. Among the three permeation steps considered in the present work, the only activated one is the transport through the Pd-based layer, whereas external mass transfer and transport in the porous support have a weaker dependency on temperature. More specifically, the external mass transfer has a functionality that is slightly lower than the linear one [43], whilst the transport in the support is even slower with increasing temperature owing to the presence of both Knudsen and viscous diffusion mechanism.

The overall results of these considerations is that a higher temperature causes the external mass transfer and the transport in the support to be relatively slower than the hydrogen transport in the metal layer, whose contribution, therefore, becomes gradually smaller and less important. The rate by which its contribution decreases with increasing temperature is quite high because the other two mechanisms increase their respective contributions at the same time.

Figure 4 shows the functionality of the step influence with another key-working condition: the hydrogen composition in mixture. It can be observed that the influence of the Pd-layer increases with increasing hydrogen feed pressure, whereas that of the external mass transfer decreases. As for the support, a non-monotone trend is found, a minimum being present at a hydrogen composition of around 0.3.

As for the external mass transfer, we can consider that the hydrogen permeating flux increases approximately linearly with hydrogen feed pressure [21]. As for the transport in the Pd-layer, we can consider that the hydrogen flux is approximately proportional to the square root of the hydrogen feed pressure. Such a functionality becomes stronger as the hydrogen feed pressure increases due to the effect of the non-ideal contribution of hydrogen diffusion in the metal lattice, which is favoured by the hydrogen pressure in a wide range of pressure conditions [21,22,44-47,49]. Therefore, as the hydrogen feed pressure increases, the external mass transfer becomes gradually faster than the transport in the Pd-layer and in the support, this resulting in the behaviour shown in Figure 4.

As for the support influence, the presence of the minimum can be understood by taking into account that, as external mass transfer

influence progressively decreases with increasing hydrogen content in the feed, the residual influence is redistributed between the Pd-layer and the support. In this redistribution, most of this residual influence gets assigned to the Pd-layer at lower hydrogen feed concentration, as the profiles in the support are less sensitive to the hydrogen content (Figure 2). Therefore, the Pd-based layer influence increases and that of the support slightly decrease.

Towards higher values of hydrogen feed content, the transport in the Pd-based layer becomes faster and, thus, the influence of the support increases, this resulting in a non-monotone trend.

Concerning the optimal membrane design, it is necessary to remark the obvious/non-obvious fact that the optimal operating conditions for membranes are those maximising the permeating flux, independently of the limiting steps controlling the permeation. From this point of view, the best case would be working under adsorption-controlled permeation [43], for which the permeating flux is just function of temperature and hydrogen partial pressure and not a function of membrane thickness.

However, working under these conditions is very difficult, if not impossible, with the actual technology, as the external mass transfer, internal diffusion and transport in the porous support are actually much slower that the hydrogen adsorption rate [43], with the second one mostly being the slowest step.

Therefore, the key-target of membrane designers is to find conditions minimising the influence of the steps external to the selective layer, whose influence is then maximised. In this particular case, the influence of the selective layer is higher towards higher hydrogen content, which actually reflects the real physical behaviour.

Figure 5 shows the trend of the step influence with membrane thickness. In this case, the effect of increasing membrane thickness is to increase the resistance of the Pd-layer, as the permeating flux under diffusion-controlled permeation is inversely proportional to membrane thickness.

As a result, the trend related to the Pd-layer increases, whereas those of the other two decrease. In this case, therefore, the minimisation of the external steps does not correspond to the flux maximisation, as membrane thickness is not kept constant in this analysis.

Furthermore, it can be observed that, going towards gradually lower values of membrane thickness, the influence of internal diffusion

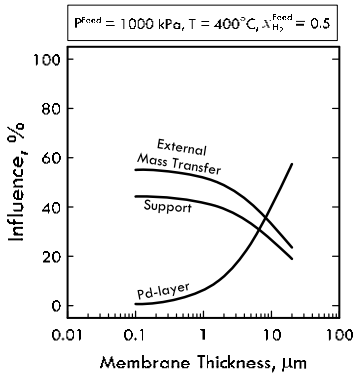

Figure 5: Step influence as a function of membrane thickness for the three permeation steps considered in this work. P^{Feed}=1000 kPa, T=400°C, x_{H2}^{Feed}=0.5.

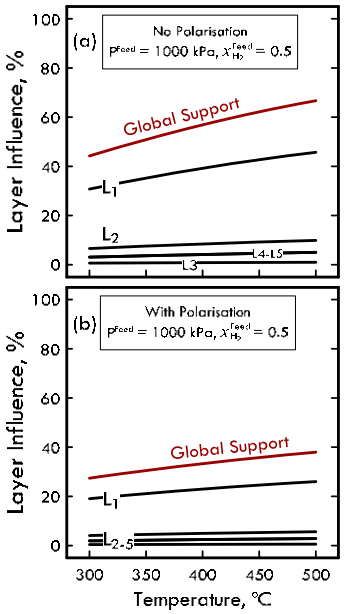

Figure 6: Influence of the support porous layers as a function of temperature in both the presence and absence of external mass transfer resistance (concentration polarisation). P^{Feed}=1000 kPa, x_{H2}^{Feed}=0.5.

tends to zero, whereas those of external mass transfer and transport in the support tend to respective constant values.

In a context where the general efforts of membrane researchers is to continuously decrease the selective layer to increase the permeating flux, this represents a useful indication to identify the lowest limit of the membrane thickness in dependence on the external operating conditions.

To analyse in a more detail the effect of the support, Figure 6 shows the influence of the different single porous layers along with that of the overall support as a function of temperature in the presence and absence of concentration polarisation for a total feed pressure of 1000 kPa and a hydrogen mole fraction of 0.5.

This type of analysis is useful to understand the bottleneck porous layers providing the largest mass transfer resistance in the support, allowing a more systematic membrane design.

From this figure, it can be observed that, in both the presence and absence of polarisation, the majority of influence is offered by the layer 1 of the support (L_1), which actually is in contact with the Pd-based selective layer. Differently, it can be considered with a good approximation that the other layers do not provide any appreciable contribution, their sum being around 4% and 8% with and without polarisation, respectively.

Moreover, by comparing Figure 6a and 6b, it is shown that polarisation reduces the influence of the support on permeation. Although the details of the physical explanation of this important fact are reported in the next section, it is here anticipated that the relative position of the mixture with respect to the support based on the flux direction plays an important role in creating an additional transport resistance causing the pressure drop in the support to be reduced.

Support resistance coefficient (SRC)

As already mentioned, it is also useful to have a single parameter

indicating the driving force loss owing to the porous support (SRC, Equations 3,4), in analogy to what done with the introduction of concentration polarisation coefficient (CPC35], which is a measure of the driving force loss in the external film on the mixture side. Let us remind that the Sieverts driving force is chosen as the characteristic one.

Figure 7 represents a map depicting the behaviour of SRC with the hydrogen mole fraction for different values of temperature and membrane thickness at a total feed pressure of 1000 kPa.

Considering a temperature of 300°C and a membrane thickness of 10 mm, starting from pure hydrogen conditions (i.e., hydrogen mole fraction equal to the unity) and going towards a gradually less hydrogen content, a decreasing SRC is observed, which means that the loss of driving force in the support is progressively smaller. Such trend can be understood by considering that, as the hydrogen feed content decreases, the influence of the external mass transfer on the feed side (i.e., concentration polarisation) increases more than that of the support, as the former is a resistance acting at first based on the flux direction. This eventually causes a driving force re-distribution in the three permeation steps considered such that there is more and more pressure drop in the external feed film rather than in the support and in a sufficiently thin Pd-based layer.

For increasing temperature, the influence of the Pd-based layer decreases, as the internal diffusion becomes faster and, at the same time, the external mass transfer on the feed side is just slightly influenced by temperature, as the gas diffusivity is not an activated process.

As well, for progressively thinner Pd-based layers, the transport through the metal lattice becomes faster and, thus, the most of pressure drop is found in the gas phase on the film side and in the support, this holding for 1 mm with a quite good approximation. This is the reason why SRC decreases faster with decreasing hydrogen content.

Concerning the information provided by the maps depicted in Figure 7, it can be observed that, although such maps provide a direct measure of the pressure drop lost in the support, the effect of external mass transfer is hidden in SRC trend. Therefore, in order to provide also such information, SRC is plotted versus CPC (Figure 8).

Considering a Pd-layer thickness of 10 mm and 300°C, SRC is observed to decrease with increasing CPC. This means that, for increasing driving force in the feed film that in the support decreases. The physical meaning of such a trend is that the effect of concentration polarisation is to decrease the effect of the porous support. This can be

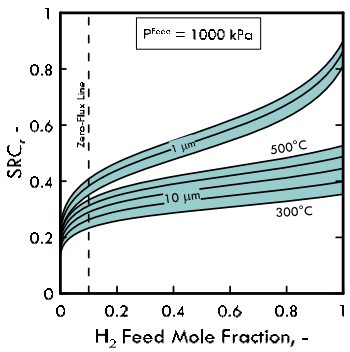

Figure 7: Support Resistance Coefficient (SRC) as a function of the hydrogen mole fraction in the feed for different values of temperature and membrane thickness. P^{Feed}=1000 kPa.

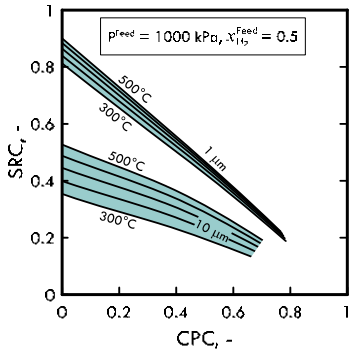

Figure 8: Support Resistance Coefficient (SRC) as a function of the Concentration Polarisation Coefficient (CPC) for different values of temperature and membrane thickness. P^{Feed}=1000 kPa, x_{H2}^{Feed}=0.5.

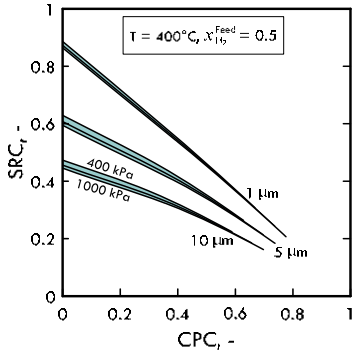

Figure 9: Support Resistance Coefficient (SRC) as a function of the Concentration Polarisation Coefficient (CPC) for different values of membrane thickness and total feed pressure. T=400°C, x_{H2}^{Feed}=0.5.

well understood by looking back at the hydrogen profiles depicted in Figure 2, where it is clear that polarisation causes a certain pressure drop before membrane, this in turn inducing a smaller pressure drop in the support, considering that the total pressure drop is determined and fixed by the users.

As a higher value of temperature is considered, SRC becomes higher at a fixed value of CPC. This is because the transport in the Pd-layer is faster whereas, at the same time, the mass transfer on the feed side is weakly influenced by temperature. Therefore, the remaining driving force is redistributed almost completely in the porous support and the sensitivity of SRC to temperature is appreciable.

On the contrary, for Pd-layers as thin as 1 mm, such sensitivity is relatively small. This occurs because, with respect to the other two permeation steps, the transport in the selective layer is fast enough that the hydrogen concentration profile can be considered almost flat, even at 300°C. In these conditions, an increasing polarisation basically causes a driving force re-distribution from the support to the feed film, this determining SRC to vary weakly with temperature than in the case at 10 mm, as the transport in the feed film does not depend on temperature (see Equation 26 reported in Caravella et al., [21]) and that in the support is a non-activated processes whose permeance actually decreases with increasing temperature.

As for the effect of the total feed pressure on SRC at a certain fixed value of hydrogen mole fraction (=0.5), Figure 9 shows that

SRC decreases with increasing total feed pressure, even though such a dependence is found to be weak for all the Pd-layer values considered. This can be understood by considering that the limiting flux related to the external mass transfer in the gas film depends weakly on the total pressure, being approximately proportional to $P^{1/3}$ (see Equation 26 reported in Caravella et al., [21]). Therefore, a higher feed pressure causes the external mass transfer in the feed to be slightly faster, whereas it does not directly affect that in the support, which, thus, becomes relatively slower for increasing feed pressure.

As a general conclusion of the presented analysis, it is withdrawn that, when membrane is used as purifier – i.e., the Pd-based layer is on the high-pressure side and the support on the permeation one – the influence of the porous support strongly depends on the concentration polarisation level.

Therefore, even if the porous support structure were optimised to minimise the mass transfer resistance, the permeation flux through thin selective layer (<10 mm ca.) would be strongly affected by concentration polarisation. Hence, a particular attention should be paid both to a correct evaluation of the overall concentration polarisation level in membrane modules [38] and to the fluid dynamics optimisation in them – like done in several design solutions studied in the literature [36,50-54] – to reduce the effect of the external mass transfer resistance in the feed side, which is found to provide the most serious pressure drop in permeation under mixture conditions.

Conclusions

In this paper, the distribution of the hydrogen permeation driving force across supported Pd-based membranes was systematically evaluated as a function of temperature, total feed pressure and selective layer thickness. For this purpose, first the influence of external mass transfer, internal diffusion and mass transport through an asymmetric five-layered porous support was calculated by using the respective permeation-limiting fluxes. This was required because of the non-linearity of the involved mass transfer resistances.

Then, the Sieverts driving force distribution across membrane was analysed by introducing a novel coefficient, here named as Support Resistance Coefficient (SRC) to quantify both the extent of the driving force lost in the support and the behaviour of its re-distribution over the other permeation steps as function of various operating conditions.

Based on the trend of such a coefficient, which was defined in analogy to the Concentration Polarisation Coefficient (CPC), it was mainly found that the concentration polarisation decreases the influence of the support on permeation. The reason for that was explained by considering that the presence of the external mass transfer resistance represents an additional barrier to permeating flux causing a first hydrogen concentration drop on the feed side that decreases that in the support.

Therefore, it is concluded that the minimisation of the support influence on permeation should be accompanied by the minimisation of the concentration polarisation as well; otherwise the expected flux increase arising from support optimisation could be relatively small in real applications.

Acknowledgements

The “Programma Per Giovani Ricercatori "Rita Levi Montalcini"” granted by the “Ministero dell’Istruzione, dell’Università e della Ricerca, MIUR” is gratefully acknowledged for funding this research.

Notation

m	Number of permeation steps
n	Number of species in mixture
J	Permeating flux, mol s^{-1} m^{-2}
P	Pressure, Pa
T	Temperature, K
x	Mole fraction

Subscripts/Superscripts:

i	Generic species in mixture
j	Generic permeation step
Lim	Limiting (flux)
Mem	Membrane

Acronyms:

CPC	Concentration Polarisation Coefficient
SRC	Support Resistance Coefficient

Greek letters:

a	Influence of a single permeation step, %

References

1. Nam SE, Lee KH (2001) Hydrogen separation by Pd alloy composite membranes: introduction of diffusion barrier. J Memb Sci 192: 177-85.
2. Su C, Jin T, Kuraoka K, Matsumura Y, Yazawa T (2005) Thin Palladium Film Supported on SiO_2-Modified Porous Stainless Steel for a High-Hydrogen-Flux Membrane. Ind Eng Chem Res 44: 3053-8.
3. Tong J, Su C, Kuraoka K, Suda H, Matsumura Y (2006) Preparation of thin Pd membrane on CeO_2-modified porous metal by a combined method of electroless plating and chemical vapor deposition. J Memb Sci 269: 101-8.
4. Bosko ML, Ojeda F, Lombardo EA, Cornaglia LM (2009) NaA zeolite as an effective diffusion barrier in composite Pd/PSS membranes. J Memb Sci 331: 57-65.
5. Li H, Goldbach A, Li W, Xu H (2007) PdC formation in ultra-thin Pd membranes during separation of H_2/CO mixtures. J Memb Sci 299: 130-7.
6. Itoh N, Akiha T, Sato T (2005) Preparation of thin palladium composite membrane tube by a CVD technique and its hydrogen permselectivity. Catal Today 104: 231-7.
7. Zhang X, Xiong G, Yang W (2008) A modified electroless plating technique for thin dense palladium composite membranes with enhanced stability. J Memb Sci 314: 226-37.
8. Peters TA, Kaleta T, Stange M, Bredesen R (2011) Development of thin binary and ternary Pd-based alloy membranes for use in hydrogen production, J Memb Sci 383: 124-134.
9. Peters TA, Kaleta T, Stange M, Bredesen R (2012) Hydrogen transport through a selection of thin Pd-alloy membranes: Membrane stability, H_2S inhibition, and flux recovery in hydrogen and simulated WGS mixtures. Catal Today 193: 8-19.
10. Lim H, Oyama ST (2011) Hydrogen selective thin palladium-copper composite membranes on alumina supports. J Memb Sci 378: 179-85.
11. Yun S, Ko JH, Oyama ST (2011) Ultrathin palladium membranes prepared by a novel electric field assisted activation. J Memb Sci 369: 482-9.
12. Dittmar B, Behrens A, Schödel N, Rüttinger M, Franco T, et al. (2013) Methane steam reforming operation and thermal stability of new porous metal supported tubular palladium composite membranes. Int J Hydrogen Energy 38: 8759-71.
13. Kanezashi M, Asaeda M (2006) Hydrogen permeation characteristics and stability of Ni-doped silica membranes in steam at high temperature. J Memb Sci 271: 86-93.
14. Kitiwan M, Atong D (2010) Effects of Porous Alumina Support and Plating Time on Electroless Plating of Palladium Membrane. J Mater Sci Technol 26: 1148-52.
15. Brunetti A, Caravella A, Fernandez E, Pacheco Tanaka DA, Gallucci F, et al.

(2015) Syngas upgrading in a membrane reactor with thin Pd-alloy supported membrane. Int J Hydrogen Energy 40: 10883-93.

16. Fernandez E, Medrano JA, Melende J, Parco M, Viviente JL, et al. (2015) Preparation and characterization of metallic supported thin Pd-Ag membranes for hydrogen separation. Chem Eng J.
17. Gallucci F, Fernandez E, Corengia P, van Sint Annaland M (2013) Recent advances on membranes and membrane reactors for hydrogen production. Chem Eng Sci 92:40-66.
18. Ward T, Dao T (1999) Model of hydrogen permeation behavior in palladium membranes. J Memb Sci 153: 211-231.
19. Catalano J, Baschetti MG, Sarti GC (2009) Influence of the gas phase resistance on hydrogen flux through thin palladium silver membranes. J Memb Sci 339: 57-67.
20. Caravella A, Barbieri G, Drioli E (2008) Modelling and simulation of hydrogen permeation through supported Pd-alloy membranes with a multicomponent approach. Chem Eng Sci 63: 2149-60.
21. Caravella A, Hara S, Drioli E, Barbieri G (2013) Sieverts Law Pressure Exponent for Hydrogen Permeation through Pd-based Membranes: Coupled Influence of Non-Ideal Diffusion and Multicomponent External Mass Transfer. Int J Hydrogen Energy 38: 16229-44.
22. Caravella A, Hara S, Sun Y, Drioli E, Barbieri G (2014) Coupled influence of non-ideal diffusion and multilayer asymmetric porous supports on Sieverts' law pressure exponent for hydrogen permeation in composite Pd-based membranes. Int J Hydrogen Energy 39: 2201-14.
23. Ryi SK, Park JS, Kim SH, Cho SH, Kim DW (2006) The effect of support resistance on the hydrogen permeation behavior in Pd–Cu–Ni ternary alloy membrane deposited on a porous nickel support. J Memb Sci 280: 883-8.
24. Gepert V, Kilgus M, Schiestel T, Brunner H, Eigenberger G, et al. (2006) Ceramic supported capillary Pd membranes for hydrogen separation: potential and present limitations. Fuel Cells 6: 472-81.
25. Huang Y, Dittmeyer R (2007) Preparation of thin palladium membranes on a porous support with rough surface. J Memb Sci 302: 160-70.
26. Huang Y, Shu S, Lu Z, Fan Y (2007) Characterization of the adhesion of thin palladium membranes supported on tubular porous ceramics. Thin Solid Films 515: 5233-40.
27. Ryi SK, Li A, Lim CJ, Grace JR (2011) Novel non-alloy Ru/Pd composite membrane fabricated by electroless plating for hydrogen separation. Int J Hydrogen Energy 36: 9335-40.
28. Sanz R, Calles JA, Alique D, Furoñes L, Ordonez S, et al. (2011) Preparation, testing and modelling of a hydrogen selective Pd/YSZ/SS composite membrane. Int J Hydrogen Energy 36: 15783-93.
29. Lee TH, Park CY, Lee G, Dorris SE, Balachandran UB (2012) Hydrogen transport properties of palladium film prepared by colloidal spray deposition. J Memb Sci 415-416:199-204.
30. Strathmann H (1981) Membrane separation processes. J Memb Sci 9: 121-189.
31. Chern RT, Koros WJ, Yui B, Hopfenberg HB, Stannett VT (1984) Selective permeation of CO_2 and CH_4 through Kapton polyimide: Effects of penetrant competition and gas phase non ideality. J Polym Sci 22: 1061-1084.
32. Rautenbach R, Albrecht R (1989) Membrane Processes. Wiley, New York.
33. Pinho MN, Semiao V, Geraldes V (2002) Integrated modeling of transport processes in fluid/nanofiltration membrane systems. J Memb Sci 206: 189-200.
34. Ahmad AL, Lau KK, Abu Bakar MZ, Shukor SRA (2005) Integrated CFD simulation of concentration polarization in narrow membrane channel. Comput Chem Eng 29: 2087-95.
35. Caravella A, Barbieri G, Drioli E (2009) Concentration polarization analysis in self-supported Pd-based membranes. Sep Purif Technol 66: 613-24.
36. Boeltken T, Belimov M, Pfeifer P, Peters TA, Bredesen R, et al. (2013) Fabrication and testing of a planar microstructured concept module with integrated palladium membranes. Chem Eng Process 67: 136-47.
37. Nekhamkina O, Sheintuch M (2016) Approximate models of concentration-polarization in Pd-membrane separators. Fast numerical analysis. J Memb Sci 500: 136-150.
38. Caravella A, Sun Y (2016) Correct Evaluation of the Effective Concentration Polarization Influence in Membrane-assisted devices. Case Study: H_2 Production by Water Gas Shift in Pd-Membrane Reactors. Int J Hydrogen Energy, In Press.
39. Caravella A, Scura F, Barbieri G, Drioli E (2010) Inhibition by CO and Polarization in Pd-Based Membranes: A Novel Permeation Reduction Coefficient. J Phys Chem B 114: 12264-76.
40. Catalano J, Giacinti Baschetti M, Sarti GC (2010) Hydrogen permeation in palladium-based membranes in the presence of carbon monoxide. J Memb Sci 362: 221-233.
41. Mejdell AL, Chen D, Peters TA, Bredesen R, Venvik HJ (2010) The effect of heat treatment in air on CO inhibition of a ~ 3 mm Pd-Ag (23 wt.%) membrane. J Memb Sci 350: 371-377.
42. Abir H, Sheintuch M (2014) Modeling H_2 transport through a Pd or Pd/Ag membrane, and its inhibition by co-adsorbates, from first principles. J Memb Sci 466: 58-69.
43. Caravella A, Scura F, Barbieri G, Drioli E (2010) Sieverts Law Empirical Exponent for Pd-Based Membranes: Critical Analysis in Pure H_2 Permeation. J Phys Chem A B 114: 6033-47.
44. Hara S, Ishitsuka M, Suda H, Mukaida M, Haraya K (2009) Pressure-dependent hydrogen permeability extended for metal membranes not obeying the square-root law. Journal of Physical Chemistry B 113: 9795-801.
45. Flanagan TB, Wang D (2010) Exponents for the Pressure Dependence of Hydrogen Permeation through Pd and Pd-Ag Alloy Membranes. J Phys Chem A C 114: 14482-8.
46. Hara S, Caravella A, Ishitsuka M, Suda H, Mukaida M, et al. (2012) Hydrogen diffusion coefficient and mobility in palladium as a function of equilibrium pressure evaluated by permeation measurement. J Memb Sci 421-422: 355-60.
47. Flanagan TB, Wang D (2012) Temperature Dependence of H Permeation through Pd and Pd Alloy Membranes. J Phys Chem A 116: 185-92.
48. Morreale BD, Ciocco MV, Enick RM, Morsi BI, Howard BH, et al. (2003) The permeability of hydrogen in bulk palladium at elevated temperatures and pressures. J Memb Sci 212: 87-97.
49. Caravella A, Hara N, Negishi H, Hara S (2014) Quantitative Contribution of Non-Ideal Permeability under Diffusion-controlled Hydrogen Permeation through Pd-membranes. Int J Hydrogen Energy 39: 4676-82.
50. Cao Z, Wiley DE, Fane AG (2001) CFD simulation of net-type turbulence promoters in a narrow channel. J Memb Sci 185: 157-76.
51. Koutsou CP, Yiantsios SG, Karabelas AJ (2004) Numerical simulation of the flow in a plane-channel containing a periodic array of cylindrical turbulence promoters. J Memb Sci 231: 81-90.
52. Geraldes V, Semiao V, Pinho MN (2003) Hydrodynamics and concentration polarization in RO/NF spiral wound modules with ladder type spacer. Desalination 157: 395-402.
53. Li F, Meindersma W, de Haan AB, Reith T (2002) Optimization of commercial net spacers in spiral wound membrane modules. J Memb Sci 208: 289-302.
54. Boeltken T, Wunsch A, Gietzelt T, Pfeifer P, Dittmeyer R (2014) Ultra-compact microstructured methane steam reformer with integrated Palladium membrane for on-site production of pure hydrogen: Experimental demonstration. Int J Hydrogen Energy 39: 18058-68.